nature medicine

ARTICLES

Correction of X-linked chronic granulomatous disease by gene therapy, augmented by insertional activation of *MDS1-EVI1*, *PRDM16* or *SETBP1*

Marion G Ott[1,16], Manfred Schmidt[2–4,16], Kerstin Schwarzwaelder[3–5,16], Stefan Stein[6,16], Ulrich Siler[7,16], Ulrike Koehl[8], Hanno Glimm[2,3], Klaus Kühlcke[9], Andrea Schilz[9], Hana Kunkel[6], Sonja Naundorf[9], Andrea Brinkmann[8], Annette Deichmann[3,4], Marlene Fischer[2,3,5], Claudia Ball[3–5], Ingo Pilz[3,5], Cynthia Dunbar[10], Yang Du[11], Nancy A Jenkins[11], Neal G Copeland[11], Ursula Lüthi[12], Moustapha Hassan[13], Adrian J Thrasher[14], Dieter Hoelzer[1], Christof von Kalle[2–4,15,16], Reinhard Seger[7,16] & Manuel Grez[6,16]

Gene transfer into hematopoietic stem cells has been used successfully for correcting lymphoid but not myeloid immunodeficiencies. Here we report on two adults who received gene therapy after nonmyeloablative bone marrow conditioning for the treatment of X-linked chronic granulomatous disease (X-CGD), a primary immunodeficiency caused by a defect in the oxidative antimicrobial activity of phagocytes resulting from mutations in gp91^{phox}. We detected substantial gene transfer in both individuals' neutrophils that lead to a large number of functionally corrected phagocytes and notable clinical improvement. Large-scale retroviral integration site–distribution analysis showed activating insertions in *MDS1-EVI1*, *PRDM16* or *SETBP1* that had influenced regulation of long-term hematopoiesis by expanding gene-corrected myelopoiesis three- to four-fold in both individuals. Although insertional influences have probably reinforced the therapeutic efficacy in this trial, our results suggest that gene therapy in combination with bone marrow conditioning can be successfully used to treat inherited diseases affecting the myeloid compartment such as CGD.

The clinical successes achieved in three phase 1/2 gene therapy studies aiming at the correction of severe combined immunodeficiencies[1–4] was partially facilitated by a selective survival and growth advantage conferred by the therapeutic gene to lymphocyte precursor cells. For many hematopoietic disorders, however, particularly those in which gene expression is crucial for effector functionality of terminally differentiated cells, bone marrow conditioning or the use of an *in vivo* selectable marker gene are thought to be key requisites for efficient engraftment and survival of gene-transduced cells. In several clinical trials conducted without bone marrow conditioning, the engraftment rate of gene-modified cells has been generally low[5–9]. This also applies for CGD, a rare inherited immunodeficiency caused by mutations in any of four genes encoding subunits of the nicotinamide dinucleotide phosphate (NADPH) oxidase complex, resulting in lack of antimicrobial activity of phagocytes[10–13]. Almost 70% of CGD cases result from defects in the X-linked gene encoding gp91^{phox} (X-CGD)[14], which together with p22^{phox} forms the heterodimeric, membrane-associated flavocytochrome b_{558}, the terminal redox center of the oxidase complex[15]. As hematopoietic stem cell (HSC) transplantation is usually indicated only for individuals with human leukocyte antigen (HLA)-matched donors[16], a reasonable therapeutic alternative for individuals with CGD is the genetic modification of autologous HSCs. Although CGD has been successfully corrected in animal models by gene transfer in HSCs[17–19], similar successes have not been achieved in humans with CGD[5,8,9].

The recent occurrence of three severe adverse events encountered in one SCID-X1 trial[20] has highlighted the risks associated with the use of integrating viruses in gene therapy[21,22]. For X-CGD, this risk was

[1]Department of Hematology/Oncology, University Hospital, Theodor-Stern-Kai 7, 60590 Frankfurt, Germany. [2]Department of Internal Medicine I, University Hospital, Hugstetterstrasse 55, 79106 Freiburg, Germany. [3]Institute of Molecular Medicine and Cell Research, Albert-Ludwigs-University, Stefan-Meier-Strasse 17, 79104 Freiburg. Germany. [4]National Center for Tumor Diseases, Im Neuenheimer Feld 350, 69120 Heidelberg, Germany. [5]Faculty of Biology, Albert-Ludwigs-University, Schaenzlestrasse 1, 79104 Freiburg, Germany. [6]Institute for Biomedical Research, Georg-Speyer-Haus, Paul-Ehrlich-Strasse 42, 60596 Frankfurt, Germany. [7]Division of Immunology/Hematology, University Children's Hospital, Steinwiesstrasse 75, 8032 Zürich, Switzerland. [8]Pediatric Hematology, Oncology and Hemostaseology, University Hospital, Theodor-Stern-Kai 7, 60590 Frankfurt, Germany. [9]European Institute for Research and Development of Transplantation Strategies (EUFETS) AG, Vollmersbachstrasse 66, 55743 Idar-Oberstein, Germany. [10]Hematology Branch, National Heart, Lung, and Blood Institute, 9000 Rockville Pike, Bethesda, Maryland 20892, USA. [11]Mouse Cancer Genetics Program, National Cancer Institute, Center for Cancer Research, 1050 Boyles Street, Frederick, Maryland 21702, USA. [12]Central Laboratory of Electron Microscopy, University of Zurich, Gloriastrasse 30, 8006 Zürich, Switzerland. [13]Department of Medicine, Division of Hematology, Karolinska Institute, SE-17177 Stockholm, Sweden. [14]Molecular Immunology Unit, Institute of Child Health, 30 Guilford Street, London WC1N 1EH, UK. [15]Cincinnati Children's Research Foundation, Molecular and Gene Therapy Program, 3333 Burnet Avenue, Cincinnati, Ohio 45229, USA. [16]M.G.O., M.S., K.S., S.S. and U.S. contributed equally to this work; C.v.K., R.S. and M.G. share senior authorship. Correspondence should be addressed to M.G. (grez@em.uni-frankfurt.de) or C.v.K. (christof.kalle@nct-heidelberg.de).

Received 7 July 2005; accepted 7 March 2006; published online 2 April 2006; doi:10.1038/nm1393

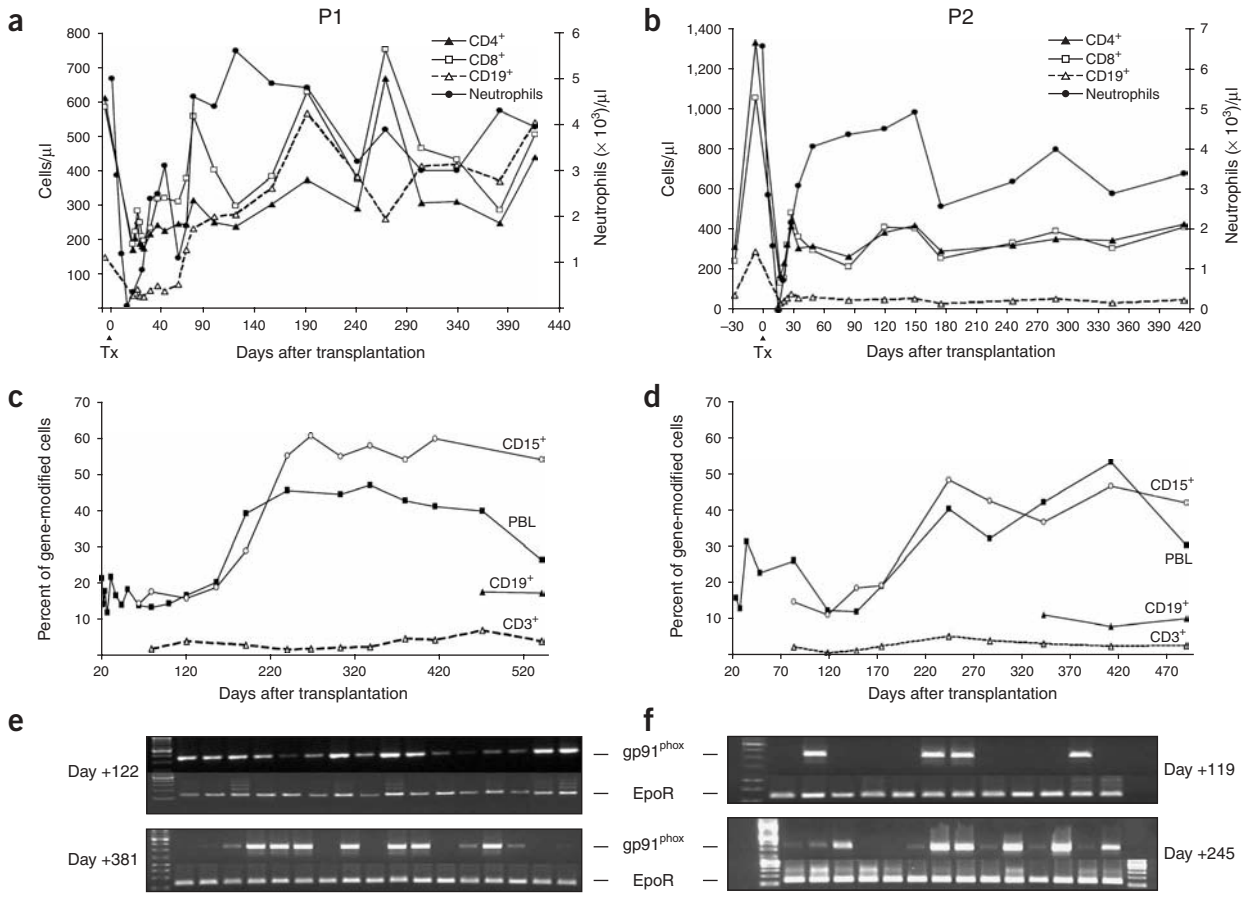

Figure 1 Hematopoietic reconstitution and gene marking in P1 and P2 after gene therapy. (**a**,**b**) Absolute neutrophil counts (right *y*-axis) and counts of helper T cells ($CD4^+CD3^+$), cytotoxic T cells ($CD8^+CD3^+$) and B cells ($CD19^+$; left *y*-axis) are shown before and after gene therapy for P1 (**a**) and P2 (**b**). Tx indicates the date of reinfusion of gene transduced cells (day 0). (**c**,**d**) Quantification of gene-modified cells in peripheral blood leukocytes (PBL), granulocytes ($CD15^+$), T-cells ($CD3^+$) and B cells ($CD19^+$) for P1 (**c**) and P2 (**d**) after gene therapy by Q-PCR. (**e**,**f**) Gene marking in CFCs derived from bone marrow aspirates of P1 (days +122 and +381; **e**) and P2 (days +119 and +245; **f**). Vector-containing CFCs were detected by PCR using primers specific for cDNA encoding $gp91^{phox}$. Input DNA was controlled by amplification of sequences derived from the human erythropoietin receptor (hEPO-R).

estimated to be low because $gp91^{phox}$ is not known to provide a survival or growth advantage to transduced cells, and abnormal hematopoiesis or leukemogenesis have never been observed in animal models of X-CGD transplanted with $gp91^{phox}$-expressing cells[18,19,23].

Here we report on two adults with X-CGD who were treated with nonmyeloablative conditioning before the infusion of genetically modified cells. Sustained engraftment of functionally corrected cells with therapeutically relevant levels of superoxide production was unexpectedly followed by *in vivo* expansion of cell clones containing insertionally activated growth-promoting genes.

RESULTS

Subjects, transduction and busulfan conditioning

We collected granulocyte colony-stimulating factor (G-CSF)–mobilized peripheral blood $CD34^+$ cells from two individuals with X-CGD aged 26 (P1) and 25 years (P2), transduced them with a monocistronic gammaretroviral vector expressing $gp91^{phox}$ ($SF71gp91^{phox}$) and reinfused them 5 d later (**Supplementary Methods** online). Transduction efficiency was 45% for P1 and 39.5% for P2, as estimated by expression of $gp91^{phox}$. The proviral copy number was 2.6 (P1) and 1.5 (P2) per transduced cell. The number of reinfused $CD34^+gp91^+$ cells per kilogram was 5.1×10^6 for P1 and 3.6×10^6 for P2. Before reinfusion, we administered liposomal busulfan (L-Bu) intravenously on days –3 and –2 every 12 h at a dose of 4 mg/kg/d. Liposomal busulfan conditioning was well tolerated by both individuals. With the exception of a grade I mucositis from day +11 to day +17 observed in P1, we observed no other nonhematological toxicities.

Both individuals experienced a period of myelosuppression (neutrophil nadir, day +14 (P1) and day +15 (P2)) with absolute neutrophil counts below 500 cells/μl between days +12 and +21 (P1) and days +13 and +18 (P2; **Fig. 1a**,**b**). We observed severe lymphopenia ($CD4^+$ cell counts, <200/μl) in P1 between days +21 and +32, whereas we observed lymphopenia in P2 only at day +17 (**Fig. 1a**,**b**). Cell counts recovered gradually to the normal values observed before busulfan conditioning (P1, 476 $CD4^+$ cells/μl, age 19; P2, 313 $CD4^+$ cells/μl, day –28). We made similar observations for $CD8^+$ and $CD19^+$ cells (**Fig. 1a**,**b** and **Supplementary Methods**).

Engraftment of gene-modified cells

We detected gene-modified cells in peripheral blood leukocytes (PBLs) from P1 at levels between 21% (day +21) and 13% (day +80; **Supplementary Methods**). From day 157, we observed a continuous increase in gene-marked cells until day +241. At that point, 46% of total leukocytes were positive for vector-encoded $gp91^{phox}$. The

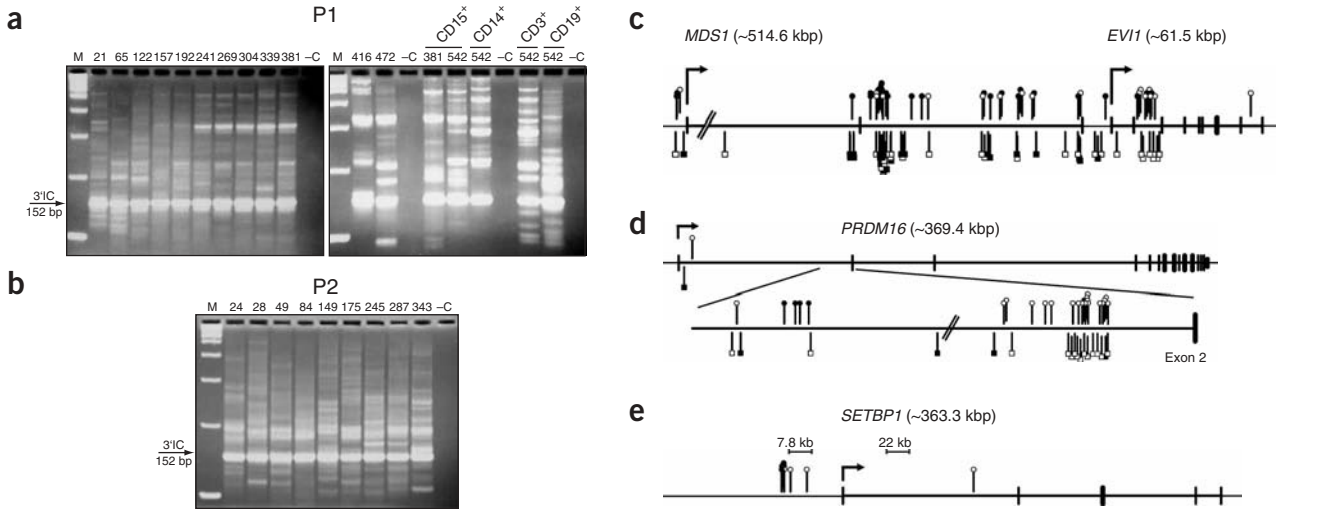

Figure 2 Polyclonal hematopoietic repopulation and non-random distribution of RIS in P1 and P2. (**a**,**b**) LAM-PCR analysis of peripheral blood leukocytes and sorted CD14$^+$, CD15$^+$, CD3$^+$ and CD19$^+$ cells (purity CD3$^+$CD19$^+$, >98%) derived from P1 21–542 d after transplantation (**a**) and P2, 24–343 d after transplantation (**b**). M, 100 bp ladder; –C, 100 ng nontransduced human genomic DNA; 3′IC, 3′-LTR internal control. (**c**–**e**) Clustering of RIS within clones sharing integrations in *MDS1-EVI1* (**c**), *PRDM16* (**d**) and *SETBP1* (**e**). Dots, RIS detected by LAM-PCR and tracking PCR in P1; squares, RIS detected by LAM-PCR and tracking PCR in P2; White symbols denote vector integration in the same orientation as gene expression, black symbols denote the reverse orientation.

percentage of gene-marked cells remained at this level until day +381 and decreased thereafter to 27% at day 542 (**Fig. 1c**). We made a similar observation in P2. The level of gene-marked leukocytes fluctuated between 31% (day +35) and 12% (day +149). Thereafter, we observed an increase in gene-marked cells with 53% of P2's leukocytes containing vector-derived sequences at day +413, which decreased again to 30% at day +491 (**Fig. 1d**).

We found vector-containing cells predominantly in the myeloid fraction. The level of gene marking in the granulocytes of P1 increased from 15% (day +65) to 55% (day +241) and fluctuated thereafter between 60% (day +269) and 54% (day +542; **Fig. 1c**). We made similar observations for P2. Whereas 15% of the granulocytes were marked at day +84, 48% of the granulocytes contained vector-derived sequences at day +245 and levels fluctuated thereafter between 36% (day +343) and 42% (day +491; **Fig. 1d**). In both subjects, the level of gene marking in CD3$^+$ cells remained low (range, 2–7% (P1) and 0.4–5% (P2)). In contrast, gene-marking levels in isolated CD19$^+$ cells of P1 (purity, >98%) were 18% (day +472) and 17% (day +542; **Fig. 1c**), whereas in B cells of P2 (purity, >94%) these values fluctuated between 11% (day +343) and 10% (day +491; **Fig. 1d**).

We estimated gene marking in bone marrow hematopoietic progenitor cells from the number of vector-positive colony-forming cells (CFCs). We detected gene-marked CFCs at a frequency of 68.8% (day +122) and 58.8% (day +381) for P1 (**Fig. 1e**), whereas these values were 33.3% (day +199) and 42.8% (day +245) for P2 (**Fig. 1f**). We detected vector-derived sequences both in colony-forming units–granulocyte-macrophage (CFU-GM; range, 63.2–76.9% (P1) and 25.0–66.6% (P2)) and burst-forming units–erythrocyte (BFU-E; range, 50.0–75% (P1), 20–40.0% (P2)) colonies, indicating effective gene marking in common myeloid progenitors with long-term engraftment capacities or in HSCs.

Distribution of retrovirus insertion sites

To study the distribution of gene-modified cells over time, we conducted a prospective large-scale mapping analysis of retrovirus insertion sites (RISs) in the subjects' cells by linear amplification-mediated PCR[24,25] (LAM-PCR; **Supplementary Methods**). We retrieved a total of 948 unique LAM-PCR RIS amplification products (P1, 551 products; P2, 397 products) by shotgun cloning and sequencing, 765 of which (P1, 435 products; P2, 330 products) could be mapped unequivocally to the human genome. Integration preferentially occurred in gene-coding regions (P1, 47%; P2, 52%) and was highly skewed toward the ±5 kb of sequence surrounding transcriptional start sites (P1, 20%; P2, 21%; **Supplementary Fig. 1** online).

RIS distribution was not stable over time and became increasingly nonrandom but still polyclonal in both subjects. The clonal contribution pattern turned into a less diverse pattern with distinct bands starting 5 months after therapy (**Fig. 2a**,**b**), indicating the appearance of multiple predominant progenitor cell clones that subsequently contributed substantially to the proportion of gene-corrected granulocytes. Sequencing of insertion loci showed that these pattern changes resulted from the emergence of clones containing an insertion in one of three genetic loci, termed common integration sites (CISs)[26] (**Supplementary Tables 1–3** online). All 134 detectable integrations at these three CISs occurred either in or near PR domain–containing zinc-finger genes *MDS1-EVI1* (91 integrations; P1, 42; P2, 49) or *PRDM16* (36 integrations; P1, 18; P2, 18) or in or near the *SETBP1* gene (7 integrations; P1, 7; P2, 0). All insertions were located in or near the upstream region of these genes, preferentially close to the transcriptional start site or internal ATG sites (**Fig. 2c–e** and **Supplementary Fig. 1**), showing an unprecedented degree of nonrandom clustering.

In vivo expansion of *MDS1-EVI1*, *PRDM16* and *SETBP1* clones

CIS clones emerged almost 3 months (P1, day +84; P2, day +80) after treatment and became predominant on day +157 (P1) and day +149 (P2). Their proportional contribution successively increased to >80% of insertions retrieved from circulating transduced cells within the next 100–150 d. The levels of contribution from the three CISs then stabilized, matching the three- to four-fold expansion of

gene-modified myelopoiesis, and plateaued without abnormal elevation of total leukocyte or neutrophil numbers (**Fig. 3a**,**b**). Individual clones showed substantial differences in their quantitative contribution over time. PCR tracking (**Supplementary Methods**) of the three CIS clones confirmed the presence of some insertions that were only detectable in one sample as well as other, more dominant clones that persistently accounted for substantial percentages of peripheral blood myeloid cells without evidence of exhaustion (**Supplementary Fig. 2** and **Supplementary Tables 1–3** online). We further analyzed dominant clones by quantitative-competitive (QC)-PCR, which confirmed their stability for a period of between 5 and 14 months after the initial expansion (**Fig. 3c**,**d** and **Supplementary Methods**).

The most productive clone in P1 contained two insertions, one in intron 2 of the *MDS1* gene locus and the other one within 18 kb downstream of *OSBPL6* and *PRKRA*. Its quantitative contribution to the pool of transduced cells increased from day +122 onward, peaked at about 80% of gene-modified cells present in the peripheral blood at day +381 and remained at that level until the last time point analyzed (day +542). We also detected this clone by QC-PCR in sorted granulocytes, B cells and T cells at day +542, indicating the

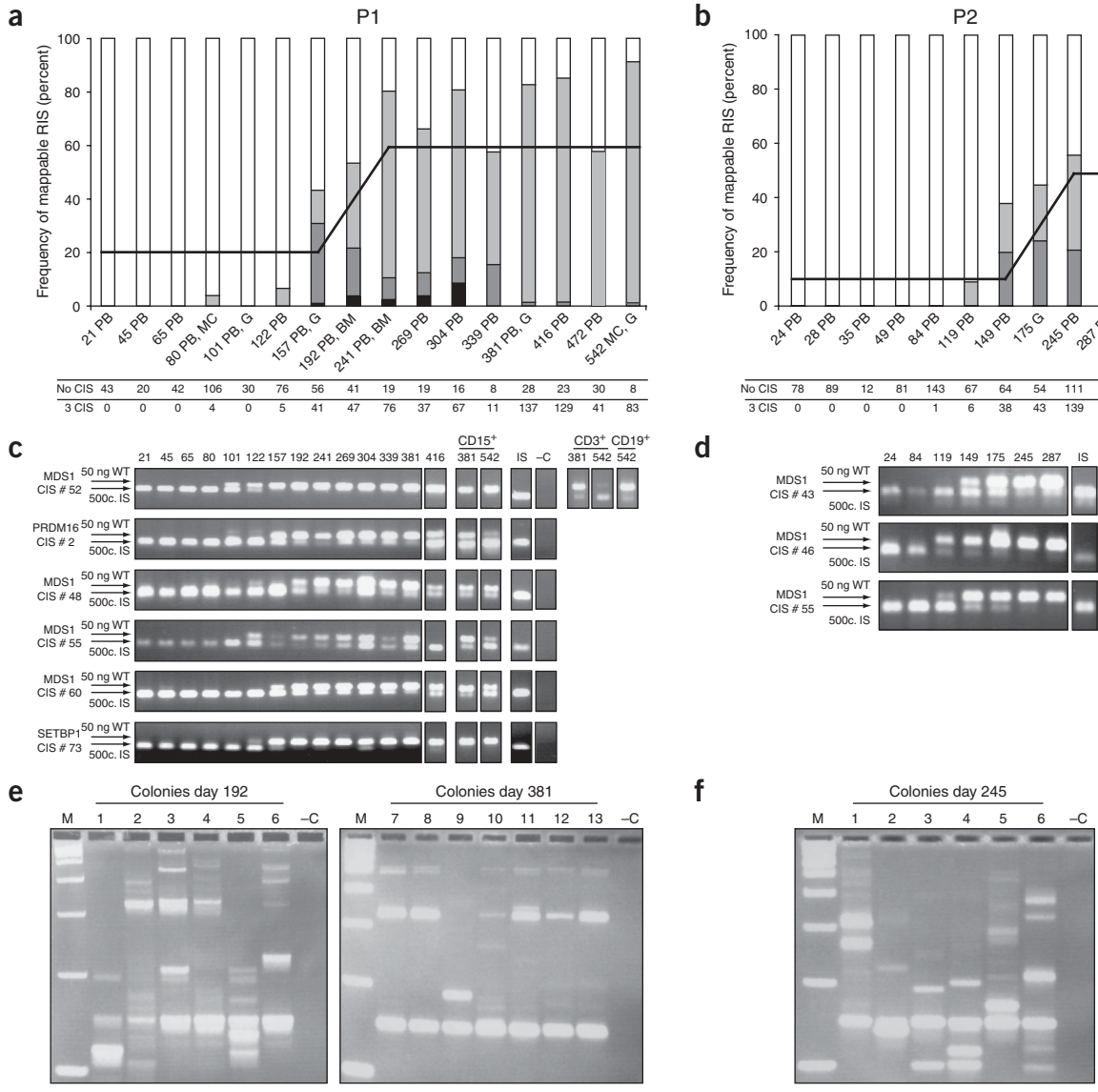

Figure 3 Insertions in *MDS1-EVI1*, *PRDM16* and *SETBP1* dominate gene-modified long-term myelopoiesis. (**a**,**b**) Overall contribution of clones with insertions in or near the three CIS-related RefSeq genes compared to all RIS locations at different time points detected in P1 (**a**) and P2 (**b**). The frequency encountered of the three CIS-related RefSeq genes *MDS1-EVI1* (light gray), *PRDM16* (dark gray) and *SETBP1* (black) in relation to non–CIS-related insertions (white) is shown as percentage of all integration site junction sequences (entire column) detected at each specific time point. In comparison, the black line denotes the approximate percentage of gene-corrected cells containing vector gp91phox among all peripheral blood granulocytes. BM, bone marrow; G, granulocytes; MC, monocytes; PB, peripheral blood. (**c**,**d**) Quantitative-competitive analysis of predominant clones from P1 (**c**) and P2 (**d**). The coamplification of 50 ng of wild-type (WT) DNA from PB in competition with 500 copies of a 26-bp deleted internal standard (IS) showed sustained contribution of all predominant clones analyzed. Numbers denote days after transplantation. –C, 50 ng nontransduced human genomic DNA. (**e**,**f**). LAM-PCR analysis of bone marrow–derived colonies from P1 at days +192 and +381 (**e**) and P2 245 d after transplant (**f**). Colony numbers 1–3, 5, 7, 9–11 and 13 are CFU-GM–derived colonies, whereas colonies 4, 6, 8 and 12 represent BFU-E colonies. M, 100 bp ladder; –C, 100 ng nontransduced human genomic DNA.

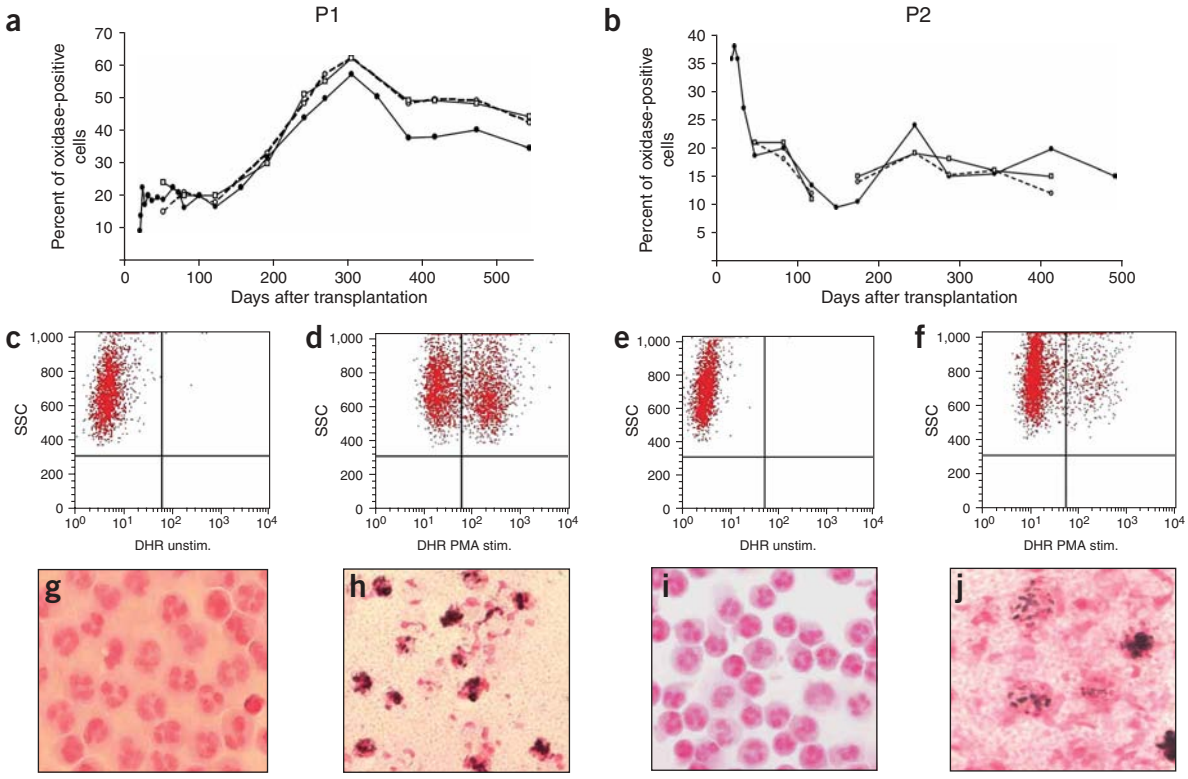

Figure 4 Functional reconstitution of NADPH oxidase activity in peripheral blood leukocytes (PBLs) and isolated granulocytes of P1 and P2 as revealed by oxidation of dihydrorhodamine (DHR) 123 (**a**–**f**) and NBT reduction (**g**–**j**). (**a**,**b**). Follow up of superoxide production in PBLs of P1 (**a**) and P2 (**b**) after stimulation with opsonized *E. coli* by DHR 123 oxidation (black dots). In parallel, superoxide production was also assessed in isolated granulocytes stimulated with PMA (open dots) or by reduction of NBT to formazan (open squares). (**c**–**f**) Examples of DHR 123 oxidation by neutrophils of P1 at day +473 and P2 at day +344 after gene therapy before (**c**,**e**) and after (**d**,**f**) PMA stimulation. (**g**–**j**) NBT reduction in single granulocytes obtained from P1 at day +381 (**g**,**h**) and P2 at day +245 (**i**,**j**) before (**g**,**i**) and after (**h**,**j**) stimulation with opsonized zymosan (OPZ).

multilineage potential of the initial transduced cells (**Supplementary Tables 1–3**). The increasing dominance of this clone could also be documented by integration-site analysis and locus-specific PCR of bone marrow progenitors (CFU-GM and BFU-E). Whereas at day +192 only 3 out of 6 (3 out of 11 by locus-specific PCR) vector-containing colonies contained the same two insertion bands, the dominant clone contributed to 6 out of 7 (28 out of 36 by locus-specific PCR) colonies at day +381 (**Fig. 3e** and data not shown). Analysis of five additional clones showed shared integration sites between $CD3^+$ cells, $CD19^+$ cells and $CD15^+$ cells obtained from P1 at days +381 and +542, again suggesting effective gene transduction of HSCs (**Figs. 2a** and **3c** and **Supplementary Tables 1–3**).

In P2, no single clone showed such a strong dominance up to day +343 (**Fig. 3f**). In line with the average of approximately 1.5–2.6 insertions per transduced cell, colonies sampled from long-term repopulating cells contained between one and four integrants per cell (**Fig. 3e**,**f**).

We obtained the highest frequency of *PRDM16*-related integration sites retrieved from P1 by LAM-PCR at day +157 (30% of the transduced-cell pool). The frequency then continuously decreased and reached 1.1% at day +542. In P2, the frequency of *PRDM16*-inserted clones decreased from day +175 (23.7%) to day +343 (12.8%). Conversely, during the same time period, the frequency of *MDS1-EVI1* integrants increased in P1 from 12% to 90.1%, and in P2 from 20.6% to 64.9%. On day +304, *SETBP1* insertions accounted for 8.4% of all integrants in P1, but from day +339 no further *SETBP1* insertions were detected by LAM-PCR. Residual activity of individual *SETBP1* clones could be detected by tracking PCR on days +381, +416, +472 and +542 (**Supplementary Tables 1–3**).

Properties of *MDS1-EVI1*, *PRDM16* and *SETBP1* clones

To confirm the functional influence of these insertions via gene activation, we analyzed specific mRNA transcripts by RT-PCR (**Supplementary Methods** online). At day +381, bone marrow cells from P1 contained substantially elevated levels of both *MDS1-EVI1* and of *SETBP1* mRNA transcripts, whereas *PRDM16* transcripts were present at levels comparable to those in control bone marrow (**Supplementary Fig. 3** online). RNA microarray analysis of the same sample confirmed overexpression of *MDS1-EVI1* or *EVI1* (36-fold) and *SETBP1* (32-fold). Abnormal expression of *PRDM16* was not found (data not shown). RT-PCR performed on RNA samples obtained from peripheral blood leukocytes of P2 at days +287 and +343 showed overexpression of *MDS1-EVI1* and *PRDM16*, whereas *SETBP1* transcripts were not detected. A microarray analysis of the same samples showed a 74-fold overexpression of *MDS-EVI1* (data not shown).

Transduced cells were strictly dependent on growth factors for proliferation and differentiation. We observed no colony formation when bone marrow mononuclear cells (P1, days +122, +192 and +241) were plated on methylcellulose and cultured for 14 d in the absence of cytokines (**Supplementary Methods**). We replated CFCs derived from $CD34^+$ cells of P1 at day +381 in the presence of cytokines into secondary and tertiary methylcellulose cultures. Only a few cell clusters were visible after the second replating, and no growth was observed in further replatings, thus indicating absence of

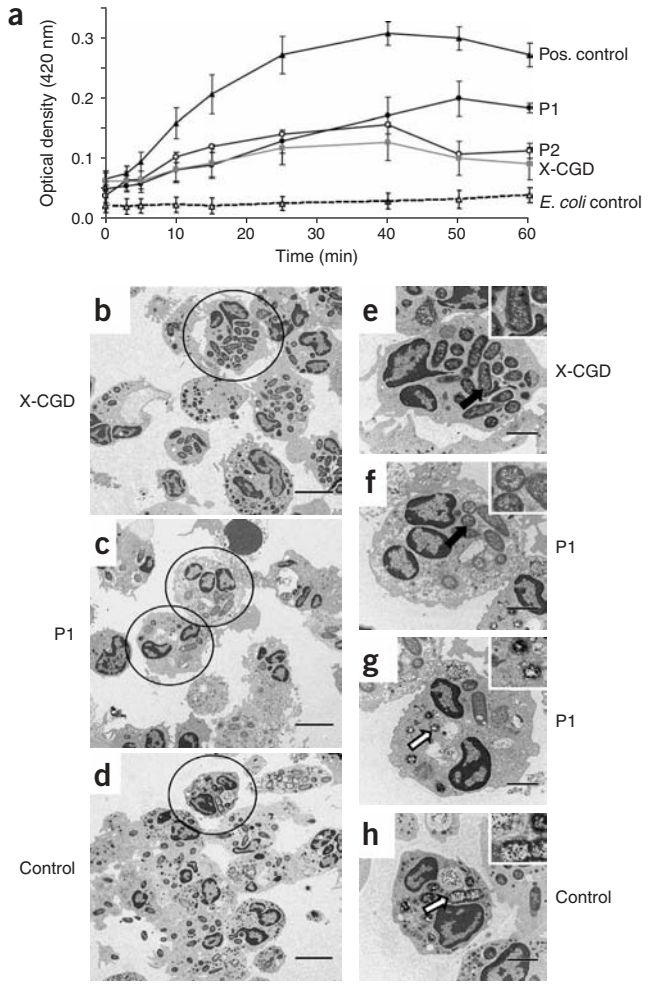

Figure 5 Antimicrobial activity of gene corrected neutrophils. (**a**) Kinetics of *E. coli* killing by neutrophils obtained from a healthy donor (positive control), P1, P2 and an individual with X-CGD compared to incubation of *E. coli* in the absence of granulocytes as a negative control. (**b**–**h**) Transmission electron microscopy of opsonized *E. coli* strain ML-35 2.5 h after phagocytosis by control (**d**,**h**), X-CGD (**b**,**e**) and P1 day +242 (**c**,**f**,**g**) granulocytes at a ratio of 10:1. Black arrows in **e** and **f** denote undigested *E. coli* inside the phagocytic vacuole. White arrows in **g** and **h** indicate *E. coli* degradation. Insert on the right upper corner shows magnifications of undigested (**e**,**f**) and digested (**g**,**h**) bacteria. Encircled areas in **b**–**d** indicate enlarged cells shown in **e**–**h**. Scale bars in **b**–**d**, 5 μm; in **e**–**h**, 2 μm.

self-renewal capacity. We obtained similar results with cells obtained from P2 at day +245 (data not shown). Furthermore, we injected 1,000 human $CD34^+$ cells derived from P1 at day +381 into each of two nude nonobese diabetic–severe combined immunodeficient (NOD-SCID) $B2m^{-/-}$ mice. We found no engraftment of $CD45^+$ cells in these mice (data not shown). Together, these data suggest that there is currently no evidence of continued abnormal growth of clones with *MDS-EVI1*, *SETBP1* or *PRDM16* integrants.

Functional reconstitution of phagocytic killing activity

We detected expression of $gp91^{phox}$ by fluorescence-activated cell sorting (FACS) using the monoclonal antibody 7D5 (ref. 27; **Supplementary Methods**). $gp91^{phox}$ was present mainly in $CD15^+$ cells with as many as 60% (P1, day +304) and 14% (P2, day +287) of the cells expressing the transgene. We found correctly assembled flavocytochrome b_{558} heterodimers by spectroscopy in cell membrane extracts from granulocytes obtained from P1 and P2. We also detected expression of $gp91^{phox}$ in bone marrow derived $CD34^+$ cells from P1 381 d after transplantation (**Supplementary Fig. 4** online).

We assayed functional reconstitution of respiratory burst activity in PBLs after stimulation with opsonized *E. coli* by the dihydrorhodamine 123 assay (**Fig. 4a**,**b** and **Supplementary Methods**). We detected NADPH oxidase activity in 10–20% of P1 leukocytes until day +122. Thereafter, we observed a strong increase in the number of oxidase-positive cells, with as many as 57% of the subject's leukocytes positive for superoxide production at day +304, followed by a decrease to 34.4% at day +542 (**Fig. 4a**). We obtained similar results with purified granulocytes after stimulation with phorbol 12-myristate 13-acetate (PMA; **Fig. 4c**,**d**) or by monitoring the reduction of nitroblue tetrazolium (NBT) to formazan in gene-corrected neutrophils (**Fig. 4g**,**h**).

The time course of superoxide production was similar in P2. The number of oxidase-positive cells was high (>35%) shortly after infusion of gene-transduced cells, but decreased to 9.6% at day +149 after transplantation. Subsequently, we observed an increase in the number of oxidase-positive cells of up to 24% (day +245; **Fig. 4b**,**e**,**f**). This value decreased to 15.3% at day +287 and fluctuated thereafter between 19.8% (day +413) and 15% (day +491). We confirmed these results by the NBT assay on individual neutrophils (**Fig. 4i**,**j**).

We quantified superoxide production in subject neutrophils by the cytochrome *c* reduction assay[28]. Total neutrophils obtained from P1 at day +193 produced 1.23 nmol superoxide/10^6 cells/min, which corresponds to 4.13 nmol/10^6 cells/min after correction for the number of oxidase-positive cells at this time point (33%). Similarly, total neutrophils from P2 at day +50 produced 2.12 nmol superoxide/10^6 gene-corrected cells/min. In comparison, the amount of superoxide produced by wild-type neutrophils was 14.35 ± 6.28 nmol superoxide/10^6 cells/min ($n = 10$; **Supplementary Fig. 5** online).

As the level of superoxide production in gene-corrected cells was at most one-third to one-seventh of the level measured in wild-type cells, we determined whether these cells would be able to kill ingested microorganisms. Bacterial killing was measured by monitoring β-galactosidase activity released by engulfed and perforated *E. coli* as previously described[29] (**Supplementary Methods**). In this assay, X-CGD cells showed minimal β-galactosidase activity as a result of impaired perforation capacity in the absence of superoxide production (**Fig. 5a**). In contrast, gene-corrected granulocytes obtained from P1 (day +473) and P2 (day +344) showed a substantial increase in β-galactosidase activity, suggesting a considerable improvement in antibacterial activity in neutrophils of both subjects after gene therapy.

We confirmed these results by electron microscopy visualization of bacterial killing by healthy, X-CGD or gene-corrected neutrophils from P1 (**Fig. 5** and **Supplementary Methods**). We observed phagocytosis of *E. coli* in all samples. The morphology of *E. coli* inside of the phagocytic vacuole, however, differed markedly between specimens. Whereas the vast majority of *E. coli* ingested by X-CGD granulocytes were not degraded (**Fig. 5b**,**e**), *E. coli* ingested by wild-type granulocytes showed clear signs of degradation as revealed by necrotic microorganisms with irregular morphology (**Fig. 5d**,**h**). Neutrophils from P1 consisted of a mixture of cells with clear bacterial degradation (**Fig. 5c**,**g**), and others without signs of bacterial degradation that were indistinguishable from noncorrected controls (**Fig. 5c**,**f**). Similarly, gene-corrected granulocytes obtained from P1 at day +381 were able to degrade *Aspergillus fumigatus* hyphae as shown by an enzymatic assay[30] and transmission electron microscopy

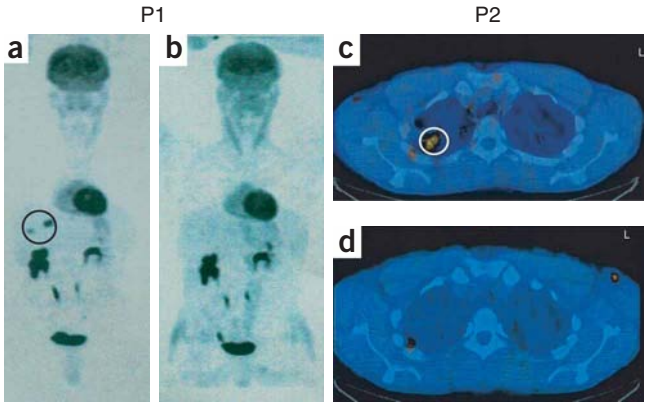

Figure 6 Fused PET scans of P1 (**a**,**b**) and fused PET-CT scans of P2 (**c**,**d**) before (**a**,**c**) and 50 (**b**) or 53 d (**d**) after gene therapy. Circle in **a** denotes two active abscesses due to *Staphylococcus aureus* infection in the liver of P1, and the circle in **c** shows ^{18}F-FDG uptake in the wall of a lung cavity of P2 due to *A. fumigatus* infection.

(**Supplementary Fig. 6** online). No killing activity could be shown in granulocytes from P2 (day +287; data not shown).

Clinical resolution of infection

The results obtained thus far suggest that gene-corrected neutrophils would potentially be able to sterilize existing bacterial and fungal infections and thus could provide a clinical benefit to the subjects. Before gene therapy, whole-body positron emission tomography (PET) scanning (**Supplementary Methods**) showed an active bacterial or fungal infection in each of the two subjects. For P1, a high focal uptake of fluorine-18-fluoro-2-deoxy-D-glucose (^{18}F-FDG) was observed in two hypodense lesions in liver segments VII/VIII and VIII, representing *Staphylococcus aureus* abscesses (**Fig. 6a**). Repeat scans performed 50 d after administration of gene-transduced cells showed no evidence of lesions in the liver of P1 (**Fig. 6b**). Similarly, P2 had suffered from severe invasive pulmonary aspergillosis due to *A. fumigatus*, visualized by ^{18}F-FDG uptake in PET scanning as a cavernous cavity extending from the apical to the posterior segment of the superior lobe on the right side (**Fig. 6c**). Only minimal ^{18}F-FDG activity was evident at day +53 after therapy in the cavity wall of P2 (**Fig. 6d**). Follow-up analysis of the subjects did not show any reappearance of these lesions. From these and other clinical parameters (**Supplementary Note** online), we conclude that gene therapy provided a therapeutic benefit to both subjects.

DISCUSSION

Previous attempts to correct human CGD by gene therapy in the absence of bone marrow ablation have been unsuccessful[5,8,9]. In contrast, substantial engraftment of gene-transduced cells and substantial gene marking in myeloid cells has been observed in gene therapy studies for adenosine deaminase–severe combined immunodeficiency (ADA-SCID) after nonmyeloablative conditioning (ref. 2 and A.J.T., personal communication). In view of these results and considering that gene-corrected CGD cells are not expected to have a proliferation or survival advantage over noncorrected cells *in vivo*, we used busulfan in a liposomal formulation (L-Bu) for conditioning of the subjects. L-Bu obviates differences arising from variable intestinal absorption, has a longer half-life in blood and marrow and is less toxic to nonhematological organs than other available forms of the drug[31,32]. We treated both subjects with antibiotics and antimycotics during the time of aplasia after chemotherapy, and thus the early resolution of the liver abscesses in P1 and the marked decrease of active aspergillosis in the lung in P2 after transplantation probably resulted from the combined action of antimicrobials and gene-transduced cells. There has been no evidence of any reappearance of these or any new lesions in CT and PET scan follow-up examinations of both subjects at later time periods. This is particularly substantial for P1 because his clinical condition made it possible to discontinue treatment with antibiotics at day +65 after transplantation.

Gene marking in peripheral blood leukocytes was sustained at levels between 10% and 30% for the first 3–4 months after transplantation. Thereafter, we observed an unexpected expansion of gene-modified cells with similar kinetics in both subjects. This may have been caused either by a direct effect of unregulated gp91^{phox} expression in progenitor cells (in which it is not normally expressed) or by long terminal repeat (LTR)-driven activation of genes involved in stem cell engraftment and/or proliferation and survival. The former consideration cannot be formally excluded, but numerous transplantation studies in X-CGD mice with gp91^{phox}-expressing cells have not shown any influence of the transgene on cell engraftment, proliferation or survival[18,19,23]. Moreover, a survey of the mouse retroviral tagged cancer gene database (RTCGD) has not shown any insertional hits affecting the gene encoding gp91^{phox}, suggesting that gp91^{phox} does not contribute to abnormal cell proliferation or even cancerogenesis in mice. By analogy to observations made in mouse models[33,34], the expansion of morphologically normal hematopoietic cells is probably caused by the activation of growth-promoting genes as a result of vector integration. The substantial numbers of clones detected as well as their predominantly myeloid differentiation pattern suggest that clonal expansion occurred mostly at an immature myeloid progenitor rather than at a stem cell level. Indeed the number of gene-marked T and B cells was low throughout the study, whereas vector-derived sequences were found predominantly in granulocytes and in granulocyte-macrophage and erythroid progenitor cells at similar frequencies. Notably, myeloid cell proliferation was restricted and did not result in granulocyte numbers exceeding those before gene therapy, suggesting that the expanded cells retained a nearly physiological response to proliferation stimuli. Similar expansion of myeloid cells has not been identified in other phase 1 studies, indicating that either the underlying disease or extrinsic factors like vector type and dosage, the source of CD34$^+$ cells (G-CSF–mobilized peripheral blood cells versus bone marrow), in combination with conditioning may influence the behavior and the fate of gene-transduced cells. In particular, the use of a vector with the spleen focus-forming virus (SFFV) LTR, which contains a potent enhancer for gene expression in hematopoietic stem and myeloid progenitor cells[35] may have influenced the outcome of our study and in particular may be responsible for the transactivation of *MDS-EVI1*, *PRDM16* and *SETBP1*.

The low level of gene marking detected in peripheral T cells may suggest transgene toxicity in the lymphoid compartment. Our own preclinical studies and data from others, however, have shown that mice repopulated with mouse HSCs transduced with gp91^{phox}-expressing vectors, including SFFV, can be repopulated to high levels with T and B cells expressing gp91^{phox} (refs. 18,19,23). This suggests to us that expression of gp91^{phox} does not impair normal lymphoid development. Thus, the lack of gene marking in peripheral T cells is probably explained by partial ablation of the lymphoid compartment and persistence of long-lived cells. In addition, it is likely that new thymopoiesis in these individuals is limited because of their age and previous disease state, as has been suggested for older individuals with SCID-X1 (ref. 36).

The insertional activation of *MDS1-EVI1* and *PRDM16* as well as *SETBP1* raises concerns that uncontrolled proliferation, abnormal hematopoiesis and eventually leukemogenesis might result from such cell clones. The constitutive overexpression of *Evi1* in mouse bone marrow cells has been shown to induce self-limiting myeloproliferation followed by a myelodysplastic syndrome (MDS) in mice[37]. Similarly, chromosomal translocations leading to deregulated *EVI1* expression have been found in human myelodysplastic syndrome and in acute and chronic myeloid leukemias[38]. The *Mds1-Evi1* gene locus also is a common target for tumorigenesis produced by wild-type retrovirus or retrovirus vector–induced insertional mutagenesis, a process that involves multiple genetic mutations[39,40].

Recently it was shown that single *Mds1-Evi1* integrations can be related to long-term *in vivo* clonal dominance that have not turned leukemic[34]. Similarly, the *MDS1-EVI1* gene is a CIS location encountered at a higher than expected frequency in a nonhuman primate gene-marking study with long-term clonal activity (median, 6 years) without clonal expansion and without signs of leukemia[41]. In addition, we have recently described transient detection of a clone with a *SETBP1* insertion in a clinical gene transfer study which has not clonally expanded in more than 7 years of follow up[42]. Moreover, the transplantation of immortalized mouse myeloid progenitor cell lines with retrovirus vector integrations in *Evi1*, *Prdm16* and *Setbp1*, similar to those found in our clinical study, did not result in engraftment or leukemia in irradiated hosts[33]. In contrast, we have found that another immortalized line containing a *Setbp1* integration can engraft and induce myeloid leukemia in mice (**Supplementary Fig. 7** and **Supplementary Note** online). The multilineage and self-renewing capacity of the founder cell may be a prerequisite for the leukemogenicity of this immortalized line, whereas less primitive cells, such as the common myeloid progenitor, may require more additional cooperating mutations before they can engraft and induce leukemia in transplanted hosts. Although we could detect six clones with shared integration sites in sorted myeloid and lymphoid cells, our functional *in vitro* and *in vivo* assays have not detected subject cell clones of similarly immature phenotype. Moreover, bone marrow cells isolated from P1 at different time points had a normal karyotype, were strictly dependent on cytokines for growth and did not engraft in xenograft animal models.

We detected sustained superoxide production in neutrophils from both subjects for more than a year. In addition to their proportion within the total neutrophil pool, the level of superoxide production per single gene-transduced cell is likely to be of crucial importance for restoration of immunity. Partial reconstitution of superoxide production in X-CGD mice as well as observations on individuals with variant CGD have indicated that the degree of protection against bacterial and fungal infections may differ depending on the level of oxidase activity[43–47]. In our study, both subjects cleared infections refractory to conventional therapy alone with levels of activity between 15% and 30% of normal activity in 20% of the circulating neutrophils. Even so, this level of correction was insufficient to avoid temporary reactivation of a chronic bacterial hidradenitis in P2, from which he had suffered for many years.

Our findings indicate that the genetic modification of human myelopoiesis is feasible and effective. Although the initial numbers of gene-corrected cells were substantial and contributed to the eradication of preexisting bacterial and fungal infections, it is difficult to predict whether these levels would have been maintained over time without the proliferative advantage conferred by retroviral insertion. Our observations now require extended prospective molecular follow up to evaluate the long-term clinical outcome and determine potential risks associated with this kind of treatment, including the probability of malignant transformation. Furthermore, our data provide clear evidence that LTR-driven retrovirus-induced gene activation occurs as a consequence of many vector insertion events and often has biological relevance for the affected cell type. This finding is of substantial importance for assessing efficacy and biosafety of gene therapy vectors in ongoing and future clinical trials.

METHODS

Subjects and clinical protocol. Subject 1 (P1, 26 years, 55 kg) was diagnosed at age 2.5 years. Mutation analysis at the *CYBB* gene locus revealed the mutation T343P within the FAD binding domain of $gp91^{phox}$, leading to the complete absence of $gp91^{phox}$ protein on the cell surface of neutrophils (phenotype $91X^{O}$). P1 was admitted to the hospital with two staphylococcal liver abscesses resistant to antibiotic treatment. Subject 2 (P2, 25 years, 75 kg) was diagnosed at birth after a positive family history. Mutation analysis revealed a 5-bp deletion in exon 10 generating a premature stop codon at amino acid 502, leading also to the phenotype $91X^{O}$. A persisting lung cavity with a thickened, PET-positive wall was detected, which was related to previous lung aspergillosis. Both subjects gave written informed consent for participation in the trial after being informed of the risks and benefits of the treatment in comparison to other available treatments. Neither subject had an HLA-identical sibling donor. The protocol was approved by the local Ethics Review Board of the University of Frankfurt Medical School and the Commission for Somatic Gene Therapy of the German Medical Council.

Collection of $CD34^+$ cells. We harvested autologous peripheral blood stem cells (PBSCs) after subcutaneous stimulation with G-CSF at a dose of 10 μg/kg/d for 6 d and collected them on a Cobe Spectra cell collector at the Blood Cell Bank in Frankfurt. $CD34^+$ progenitor cells were immunomagnetically selected on CliniMacs columns (Miltenyi Biotec) following GMP rules. The initial $CD34^+$ cell numbers were 1.6×10^8 for P1 and 3.5×10^8 for P2.

Conditioning and clinical follow up. We performed nonmyeloablative conditioning by administration of liposomal busulfan every 12 h at 4 mg/kg/d on days −3 and −2. The interval between the last L-Bu dose and stem cell reinfusion was 48 h. L-Bu bioavailability was similar for both subjects, as shown by the area under the curve (AUC) of the plasma concentration time curve resulting in a median value for the first and third dose of 11,824 ± 229.1 and 12,545 ± 1,126.42 ng × h/ml for P1 and P2, respectively. Under standard antiemetic prophylaxis, no nausea and vomiting occurred, and no signs of anorexia, of higher levels of hepatic enzymes or of retention parameters, of central nervous system toxicity (seizures) or changes in lung function were documented during or after busulfan conditioning in either subject. P1 and P2 experienced complete but reversible alopecia. The duration of severe neutropenia (<500 cells/μl) was 9 and 5 d for P1 and P2, respectively, whereas lymphopenia ($CD4^+$ cell counts <200 cells /μl) lasted 11 d for P1 and only 1 d for P2, thereby limiting the likelihood of the reactivation of viral infections, one of the major complications of allogeneic bone marrow transplantation. During chemotherapy and the following 30 d, P1 received oral clindamycin, cefalexin and rifampicin for treatment of liver abscesses, and received cotrimoxazol and itraconazol as prophylactic standard therapy. Similarly, P2 received oral cotrimoxazol, rifampicin and intravenous cefotaxim for prophylactic therapy and received liposomal amphotericin intravenously for treatment of aspergillosis. P1 received one blood (day +14) and two platelet (days +15 and +20) transfusions, P2 received one blood and one platelet transfusion on day +15 as prophylactic treatment during pancytopenia after chemotherapy. The subjects left the hospital at day +33 (P1) and day +27 (P2).

After transplantation, each subject has had one episode of a mild mycoplasma infection (serological positivity, no direct demonstration of bacteria in the bronchoalveolar lavage) without fever. In P1, a mycoplasma and *Bordetella pertussis* bronchitis was diagnosed at day +463. Until this time point, he had received no prophylactic antifungal and antimicrobial therapy. The infection was treated at home with an oral antibiotic. In P2, a mycoplasma pneumonia and sinusitis maxillaris was diagnosed at day +149. This subject was under prophylactic antibiotic care with cotrimoxazol and was treated at

home with a standard antibiotic. Both subjects have been free of severe bacterial and fungal infections and have not been hospitalized for such episodes since transplantation.

Note: Supplementary information is available on the Nature Medicine website.

ACKNOWLEDGMENTS

We are indebted to families of the subjects for their continuous support and to the medical and nursing staff of the bone marrow transplantation unit of the Department of Hematology at the University Hospital in Frankfurt. We thank E. Karaus, M. Rutishauser and C. Wenk (University Children's Hospital, Zurich) for technical assistance with the granulocyte function tests, L. Chen (Georg-Speyer-Haus, Frankfurt) for valuable help during monitoring of the subjects, S. Wehner, R. Quaritsch, S. Grohal, R. el Kaláoui and C. Kramm (University Children's Hospital, Frankfurt) for assistance with granulocyte tests and immunophenotyping, and S. Schmidt, S. Fessler, C. Prinz, M. Wissler, S. Braun and R. Cziumplik (University of Freiburg) for technical assistance with the molecular analysis. Special thanks to D. Pfeifer (University Hospital Freiburg) for performing the microarray analysis. We are also grateful to T. Bächi (Central laboratory for electron microscopy, University of Zurich) for electron microscopic analysis, to H. Steinert (Nuclear Medicine Clinic, University Hospital Zurich, Switzerland) for PET-CT scans and D. Roos (Sanquin, Department of Experimental Hematology, The Netherlands) for advice with the *E. coli* killing assays. We also thank C. Baum (Hannover Medical School) and K. Cichutek (Paul-Ehrlich-Institute) for the gift of materials and discussions during this work. RetroNectin (CH-296) was provided by Takara Bio Inc. This work was supported by the Swiss National Science Foundation (National Research Program on Somatic Gene Therapy NFP 37), by the German Ministry of Education and Research (grants 01GE9634/2 and 01GE9904), by the CGD Research Trust, London (grant J4G/01/01), by the European Union (Sixth Framework Program, CONSERT) and by Deutsche Forschungsgemeinschaft grants Ka976/5-3 and Ka976/6-2. A.J.T. is supported by the Wellcome Trust. The Georg-Speyer-Haus is supported by the Bundesministerium für Gesundheit and the Hessisches Ministerium für Wissenschaft und Kunst.

COMPETING INTERESTS STATEMENT

The authors declare that they have no competing financial interests.

Published online at http://www.nature.com/naturemedicine/
Reprints and permissions information is available online at http://npg.nature.com/reprintsandpermissions/

1. Cavazzana-Calvo, M. *et al.* Gene therapy of human severe combined immunodeficiency (SCID)-X1 disease. *Science* **288**, 669–672 (2000).
2. Aiuti, A. *et al.* Correction of ADA-SCID by stem cell gene therapy combined with nonmyeloablative conditioning. *Science* **296**, 2410–2413 (2002).
3. Hacein-Bey-Abina, S. *et al.* Sustained correction of X-linked severe combined immunodeficiency by *ex vivo* gene therapy. *N. Engl. J. Med.* **346**, 1185–1193 (2002).
4. Gaspar, H.B. *et al.* Gene therapy of X-linked severe combined immunodeficiency by use of a pseudotyped gammaretroviral vector. *Lancet* **364**, 2181–2187 (2004).
5. Malech, H.L. *et al.* Prolonged production of NADPH oxidase-corrected granulocytes after gene therapy of chronic granulomatous disease. *Proc. Natl. Acad. Sci. USA* **94**, 12133–12138 (1997).
6. Dunbar, C.E. *et al.* Retroviral transfer of the glucocerebrosidase gene into CD34$^+$ cells from patients with Gaucher disease: *in vivo* detection of transduced cells without myeloablation. *Hum. Gene Ther.* **9**, 2629–2640 (1998).
7. Kohn, D.B. *et al.* T lymphocytes with a normal ADA gene accumulate after transplantation of transduced autologous umbilical cord blood CD34$^+$ cells in ADA-deficient SCID neonates. *Nat. Med.* **4**, 775–780 (1998).
8. Malech, H.L., Choi, U. & Brenner, S. Progress toward effective gene therapy for chronic granulomatous disease. *Jpn. J. Infect. Dis.* **57**, 27–28 (2004).
9. Barese, C.N., Goebel, W.S. & Dinauer, M.C. Gene therapy for chronic granulomatous disease. *Expert Opin. Biol. Ther.* **4**, 1423–1434 (2004).
10. Roos, D. The genetic basis of chronic granulomatous disease. *Immunol. Rev.* **138**, 121–157 (1994).
11. Segal, A.W. The NADPH oxidase and chronic granulomatous disease. *Mol. Med. Today* **2**, 129–135 (1996).
12. Segal, B.H., Leto, T.L., Gallin, J.I., Malech, H.L. & Holland, S.M. Genetic, biochemical, and clinical features of chronic granulomatous disease. *Medicine (Baltimore)* **79**, 170–200 (2000).
13. Heyworth, P.G., Cross, A.R. & Curnutte, J.T. Chronic granulomatous disease. *Curr. Opin. Immunol.* **15**, 578–584 (2003).
14. Winkelstein, J.A. *et al.* Chronic granulomatous disease. Report on a national registry of 368 patients. *Medicine (Baltimore)* **79**, 155–169 (2000).
15. Babior, B.M. NADPH oxidase. *Curr. Opin. Immunol.* **16**, 42–47 (2004).
16. Seger, R.A. *et al.* Treatment of chronic granulomatous disease with myeloablative conditioning and an unmodified hemopoietic allograft: a survey of the European experience, 1985–2000. *Blood* **100**, 4344–4350 (2002).
17. Mardiney, M., 3rd *et al.* Enhanced host defense after gene transfer in the murine p47phox-deficient model of chronic granulomatous disease. *Blood* **89**, 2268–2275 (1997).
18. Dinauer, M.C., Li, L.L., Bjorgvinsdottir, H., Ding, C. & Pech, N. Long-term correction of phagocyte NADPH oxidase activity by retroviral-mediated gene transfer in murine X-linked chronic granulomatous disease. *Blood* **94**, 914–922 (1999).
19. Sadat, M.A. *et al.* Long-term high-level reconstitution of NADPH oxidase activity in murine X-linked chronic granulomatous disease using a bicistronic vector expressing gp91phox and a Delta LNGFR cell surface marker. *Hum. Gene Ther.* **14**, 651–666 (2003).
20. Hacein-Bey-Abina, S. *et al.* LMO2-associated clonal T cell proliferation in two patients after gene therapy for SCID-X1. *Science* **302**, 415–419 (2003).
21. Baum, C. *et al.* Chance or necessity? Insertional mutagenesis in gene therapy and its consequences. *Mol. Ther.* **9**, 5–13 (2004).
22. von Kalle, C. *et al.* Stem cell clonality and genotoxicity in hematopoietic cells: gene activation side effects should be avoidable. *Semin. Hematol.* **41**, 303–318 (2004).
23. Bjorgvinsdottir, H. *et al.* Retroviral-mediated gene transfer of gp91phox into bone marrow cells rescues defect in host defense against *Aspergillus fumigatus* in murine X-linked chronic granulomatous disease. *Blood* **89**, 41–48 (1997).
24. Schmidt, M. *et al.* Polyclonal long-term repopulating stem cell clones in a primate model. *Blood* **100**, 2737–2743 (2002).
25. Schmidt, M. *et al.* Clonality analysis after retroviral-mediated gene transfer to CD34$^+$ cells from the cord blood of ADA-deficient SCID neonates. *Nat. Med.* **9**, 463–468 (2003).
26. Suzuki, T. New genes involved in cancer identified by retroviral tagging. *Nat. Genet.* **32**, 166–174 (2004).
27. Yamauchi, A. *et al.* Location of the epitope for 7D5, a monoclonal antibody raised against human flavocytochrome b558, to the extracellular peptide portion of primate gp91phox. *Microbiol. Immunol.* **45**, 249–257 (2001).
28. Mayo, L.A. & Curnutte, J.T. Kinetic microplate assay for superoxide production by neutrophils and other phagocytic cells. *Methods Enzymol.* **186**, 567–575 (1990).
29. Hamers, M.N., Bot, A.A., Weening, R.S., Sips, H.J. & Roos, D. Kinetics and mechanism of the bactericidal action of human neutrophils against *Escherichia coli*. *Blood* **64**, 635–641 (1984).
30. Rex, J.H., Bennett, J.E., Gallin, J.I., Malech, H.L. & Melnick, D.A. Normal and deficient neutrophils can cooperate to damage *Aspergillus fumigatus* hyphae. *J. Infect. Dis.* **162**, 523–528 (1990).
31. Hassan, M. *et al.* Pharmacokinetics and distribution of liposomal busulfan in the rat: a new formulation for intravenous administration. *Cancer Chemother. Pharmacol.* **42**, 471–478 (1998).
32. Hassan, Z. *et al.* Pharmacokinetics of liposomal busulphan in man. *Bone Marrow Transplant.* **27**, 479–485 (2001).
33. Du, Y., Jenkins, N.A. & Copeland, N.G. Insertional mutagenesis identifies genes that promote the immortalization of primary bone marrow progenitor cells. *Blood* **106**, 3932–3939 (2005).
34. Kustikova, O. *et al.* Clonal dominance of hematopoietic stem cells triggered by retroviral gene marking. *Science* **308**, 1171–1174 (2005).
35. Baum, C., Hegewisch-Becker, S., Eckert, H.G., Stocking, C. & Ostertag, W. Novel retroviral vectors for efficient expression of the multidrug resistance (mdr-1) gene in early hematopoietic cells. *J. Virol.* **69**, 7541–7547 (1995).
36. Thrasher, A.J. *et al.* Failure of SCID-X1 gene therapy in older patients. *Blood* **105**, 4255–4257 (2005).
37. Buonamici, S. *et al.* EVI1 induces myelodysplastic syndrome in mice. *J. Clin. Invest.* **114**, 713–719 (2004).
38. Johansson, B., Fioretos, T. & Mitelman, F. Cytogenetic and molecular genetic evolution of chronic myeloid leukemia. *Acta Haematol.* **107**, 76–94 (2002).
39. Li, Z. *et al.* Murine leukemia induced by retroviral gene marking. *Science* **296**, 497 (2002).
40. Buonamici, S., Chakraborty, S., Senyuk, V. & Nucifora, G. The role of EVI1 in normal and leukemic cells. *Blood Cells Mol. Dis.* **31**, 206–212 (2003).
41. Calmels, B. *et al.* Recurrent retroviral vector integration at the MDS1–EVI1 locus in rhesus long-term repopulating hematopoietic stem cells. *Blood* **106**, 2530–2533 (2005).
42. Glimm, H. *et al.* Efficient marking of human cells with rapid but transient repopulating activity in autografted recipients. *Blood* **106**, 893–898 (2005).
43. Dinauer, M.C., Gifford, M.A., Pech, N., Li, L.L. & Emshwiller, P. Variable correction of host defense following gene transfer and bone marrow transplantation in murine X-linked chronic granulomatous disease. *Blood* **97**, 3738–3745 (2001).
44. Mills, E.L., Rholl, K.S. & Quie, P.G. X-linked inheritance in females with chronic granulomatous disease. *J. Clin. Invest.* **66**, 332–340 (1980).
45. Johnston, R.B., 3rd, Harbeck, R.J. & Johnston, R.B., Jr. Recurrent severe infections in a girl with apparently variable expression of mosaicism for chronic granulomatous disease. *J. Pediatr.* **106**, 50–55 (1985).
46. Rosen-Wolff, A. *et al.* Increased susceptibility of a carrier of X-linked chronic granulomatous disease (CGD) to *Aspergillus fumigatus* infection associated with age-related skewing of lyonization. *Ann. Hematol.* **80**, 113–115 (2001).
47. Wolach, B., Scharf, Y., Gavrieli, R., de Boer, M. & Roos, D. Unusual late presentation of X-linked chronic granulomatous disease in an adult female with a somatic mosaic for a novel mutation in CYBB. *Blood* **105**, 61–66 (2005).

Supplementary Note

Clinical history of P1 and P2 before and after gene therapy

First diagnosis of X-CGD in patient P1 was done in 1981. He suffered from severe bacterial and fungal infections as well as granuloma of the ureter with stenosis, pyeloplastic operation (1978), liver abscesses (1980), pseudomonassepticemia (1985), candida-oesophagitis(1992), salmonellasepticemia (1993), severe osteomyelitis, spondylitis with epidural and paravertebral abscess and corporectomy (June 2002). Since 2003 severe therapy-resistant liver abscesses (Staph aureus) were diagnosed. On admission to the hospital in Frankfurt, the patient was treated with clindamycin, cefalexin, cotrimoxazol and itraconazol, the later two as standard long-term prophylaxis. We changed clindamycin to rifampicin orally. After gene therapy and resolution of the liver abscesses we removed rifampicin (day +65) and kept the standard prophylactic care with itraconazol. During the follow-up and concomitant increase in gene marked cells with effective killing of *Aspergillus fumigatus* we removed also itraconazol (day +381). No reappearance of liver abscesses and no positive bacterial culture were observed until the last monitoring time point. The patient had a net weight gain of 10 kg since transplantation and a marked decrease of lung granulomas in the CT scan. Lung function is stable.

First diagnosis of X-CGD for patient P2 was in 1979. He suffered from cervical lymphnode abscesses (1983), meningitis (1985), parotis abscesses (1990), two liver abscesses, cervical lymphnode abscesses (1991 and 1992), sinusitis maxillaris (1995), bilateral hidradenitis axillaris and pneumonia (2000). Since 2002 he was suffering from bilateral lung aspergillosis with cerebral emboli and formation of a lung cavity. The patient was admitted to the hospital treated by voriconazol and cotrimoxazol. After gene therapy a complete resolution of the aspergillosis was

observed, but no improvement in lung function due to excess abuse of nicotine. The patient developed a mycoplasma pneumonia (positive serological IgM titers, no antigen positivity in serum and sputum, negative culture after bronchoalveolar lavage) and sinusitis maxillaris on day +149. He was treated with oral clindamycin for 3 weeks. During gene therapy and busulfan treatment, we changed voriconazol to liposomal amphotericin B until day +23. We restarted voriconazol on day +24. No hospital admissions after gene therapy and no positive bacterial cultures were observed. P2 is still under cotrimoxazole/voriconazole prophylaxis because the number of oxidase positive cells and the amount of superoxide production per cell were less than 20%. Moreover killing of *A. fumigatus* could not be demonstrated in vitro.

Clinical parameters after gene therapy

BM cellularity

Bone marrow aspirates of both patients were routinely examined at several time points (P1: days +122, +192, +241, +381; P2: days +84, +119, +245). Following analyses were done: morphology (Pappenheim staining) was normal at all time points and showed a completely normal hematopoesis, normal cellularity, normal megakaryo, erythro- and granulopoesis and no signs of leukemia. One example each is described below: P1 day +381: megakaropoesis normal, X-cell 1%, promyelocytes 8%, myelocytes 16%, metamyelocytes and bands 14%, segmented 15%, eosinophils 6%, basophils 1%, monocyte 3%, erythroblasts 21%, plasma cells 2%, lymphoids 12%. P2 day +245: megakaryopoesis normal, promyelocytes 10%, myelocytes 19%, metamyelocytes and bands 12%, segmented 11%, eosinophils 4%, basophils 1%, monocytes 3%, erythroblast 26%, plasma cells 4%, lymphoids 10%.

CFU-C content

Bone marrow aspirates were taken at days +122, +192, +241 and +381 for P1 and at days +84, +119 and +245 for P2. On each occasion a bone marrow total BM mononuclear cells were plated on methylcellulose (Methocult, Stem Cells Technologies) and colony formation was assessed 14 days later. Table 1 shows a summary of these data

Table 1.

P1	CFU-GM per 10^5 cells	BFU-E per 10^5 cells
Day +122	25	24
Day +192	25	33
Day +241	49	55
Day +381	70	133
Day +381 $CD34^+$ (10^3)	29	60
P2		
Day + 84	49	88
Day +119	73	72
Day +245	153	52
Day +245 $CD34^+$ (10^3)	42	12

Immunophenotyping

Immunophenotyping of bone marrow cells performed by FACS analysis with antibodies against CD19, CD10, CD10/CD19, CD34, CD33 and CD34/CD33 showed no abnormal expression profile or cell counts in either patient at any time.

Immunohistostaining

Immunohistostaining of bone marrow biopsies for CD10, CD34, CD117, CD3, and CD20 was performed at day +381 (P1) and day +491 (P2). No infiltration of blast cells, no myelo- or lymphoproliferative disease and no myelodyplastic syndrome were seen in these preparations.

BM cytogenetics

Cytogenetic analysis were performed at the Department of Molecular Pathology, University Medical School, Hannover, Germany under the direction of Prof. Dr. med. B. Schlegelberger. Following samples were analyzed: P1: day +241 (16 metaphases), day +381 (18 metaphases); P2 day +119 (15 metaphases), day +245 (21 metaphases). In all cases a normal karyotype was observed.

T-cell function

Mononuclear cells obtained at different time points from P1 and P2 were stimulated with diverse mitogens and antigens. Proliferative responses were assayed by ^{3}H-Thymidine incorporation. The ratio of ^{3}H-Thymidine incorporation in mitogen- or antigen stimulated vs. non-stimulated cells is given in **Table 1** as a quotient. In all cases, robust incorporation of ^{3}H-Thymidine were observed, indicating that the mitogen and antigen responses of patient lymphocytes are within the range of age-matched healthy individuals. Also, immunoscope analysis of Vß T lymphocytes at day +245 (P1) and day +491 (P2) showed normal T cell receptor repertoires in both patients.

Table 1.

Lymphocyte function P1	**Before GT**	**Quotient day +53**	**Quotient day +597**	**Control**
Mitogens				
PHA	302	167-183	57-59	>30
Staphylococcus Enterotoxin		136	54	>30
Anti-CD3		109	52	>30
PMA + Ionomycin		109	32-36	>30
Antigens				
Candida albicans		12-17	164-175	>10
Cytomegalovirus		14-18	2	>10
Tuberculin (purified protein derivate)		17	183	>10
Tetanus	63	22-31	78-88	>10
Lymphocyte function P2	**Before GT**	**Quotient day +50**		**Control**
PHA	482-514	114-152		>30
Staphylococcus Enterotoxin	370	283		>30
Anti-CD3	496	210		>30
PMA + Ionomycin	506	95		>30

Antibody production

Among others normal levels of IgG, IgA, IgM, IgG1, IgG2, IgG3 and IgG4 were found. Examples of plasma protein levels are shown below at days +546 (P1) and day +489 (P2).

P1	**Before GT**	**After GT day +546**	**Control range**
IgG	995 mg/dl	1140 mg/dl	700-1600
IgA	218 mg/dl	364 mg/dl	70-400
IgM	143 mg/dl	57 mg/dl	40-230
P2	**Before GT**	**After GT day +489**	**Control range**
IgG	1678 mg/dl	1140 mg/dl	700-1600
IgA	537 mg/dl	383 mg/dl	70-400
IgM	254 mg/dl	87.2 mg/dl	40-230

Similarly, IgG antibodies against Tetanus Toxoid (610 U/l), Diphteria Toxoid (270 U/l) and Hemophilus influenzae Typ B (3.10 µg/ml) were detected at day 597 in serum samples of P1.

Mouse integration and transplantation data related to our clinical study.

More than 80 immortal cell clones were generated after retroviral transduction of murine bone marrow cells in the presence of SCF and IL3, of which some have been maintained in culture for more than 1.5 years. The majority of these clones had a phenotype similar to committed immature myeloid progenitors and were still IL-3 dependent. All karyotypes were found to be normal. Spontaneous differentiation of the cultures yielded neutrophils (10-40%) and macrophages (1-5%). 95% of cells could be differentiated into neutrophils in response to G-CSF, whereas GM-CSF

treatment induced differentiation into macrophages (30%) and neutrophils (70%). Addition of PMA induced 50-70% of cells to differentiate into macrophages. Integration sites have been analyzed in 37 clones, demonstrating 1 to 7 integrants per cell. 7 cell clones showed integrants in the *Evi1* gene locus, 13 in the *Prdm16* gene region and 1 in Setbp1. Notably, northern analysis showed that expression of *Evi1* and *Prdm16* was mutually exclusive[1].

The engraftment potential of these immortalized cell lines was also tested. 2-8×10^6 Ly5.1$^+$ cells from *Evi1* (two clones), *Prdm16* (one) and *Setbp1* (one) immortalized cell lines, together with 5×10^5 unirradiated C57BL/6-Ly5.2$^+$ supporting bone marrow cells, failed to engraft lethally irradiated C57BL/6-Ly5.2$^+$ mice.

Further, 10 immortalized early hematopoietic progenitor cell clones have been produced by retroviral transduction in the presence of SCF and FLT3 ligand. Of these, one (SF-1) revealed a very immature phenotype (Sca-1-, 50% c-kit+) with lymphomyeloid differentiation capacity and an integration in *Setbp1*. In contrast to the immortalized clones with the committed myeloid progenitor phenotype, transplantation of 2.5-5.6×10^6 Ly5.1$^+$ SF-1 cells did result in a leukemic phenotype. All eleven hosts died of leukemia 56-118 days post transplant. Secondary recipients of 1×10^6 leukemic cells developed leukemias 30 days after transplantation. This SF-1 cell line revealed two integrants, one located at an unknown gene locus (without abnormal gene expression) and one in intron 1 of *Setbp1*. The leukemic potential of SF-1 cells is very likely related to the immature phenotype of the clone (engraftment and self-renewal capacity).

In summary, immortalized early hematopoietic progenitor cells can induce leukemias in transplanted hosts whereas immortalized immature myeloid cells can not, suggesting that a leukemic outcome can occur from primitive cells immortalized after *in vitro* transduction.

In our clinical study, we could not detect any *SETBP1* integrant in P2 (and no *SETBP1* overexpression). In contrast, seven integrants into *SETBP1*, six located ~20kb upstream and one in intron 1 of the gene, were detected in P1. The position of the integrant in intron 1 was similar to the two integrants found in the mouse study. This particular clone (77509D02) was detected only once by LAM-PCR in peripheral blood of P1 at day +241, but could not be detected at any other time point by tracking PCR (**Supplementary Tables** online).

Acknowledgments

We thank M. Eyrich (University Children´s Hospital, Würzburg) for analysis of T-cell receptor repertoires and R. Schubert (University Children´s Hospital, Frankfurt) for proliferation assays.

References

1. Du, Y., Jenkins, N.A. & Copeland, N.G. Insertional mutagenesis identifies genes that promote the immortalization of primary bone marrow progenitor cells. *Blood* **106**, 3932-3939 (2005).